Int. Agrophysics, 2006, 20, 207-218

INTERNATIONAL
Agrophysics
www.ipan.lublin.pl/int-agrophysics

Limited entrapment model to simulate the breakthrough of *Arthrobacter* and *Aquaspirillum* in soil columns**

Y.A. Pachepsky[1]*, *B.A. Devin*[2], *L.M. Polyanskaya*[3], *D.R. Shelton*[1], *E.V. Shein*[3], *and A.K. Guber*[4]

[1]USDA-ARS Environmental Microbial Safety Laboratory, Beltsville, MD, USA
[2]Moscow State University – Russian Academy of Sciences, Soil Science Institute, Moscow, Russia
[3]Lomonosov Moscow State University, Department of Soil Science, Moscow, Russia
[4]Department of Earth and Environmental Sciences, University of California, Riverside, USA

Received February 13, 2006; accepted May 23, 2006

A b s t r a c t. Bacterial transport through soils is attracting more attention because soil serves as an environmental bacterial filter, thereby reducing microbial contamination of ground water. We conducted a series of transport experiments, using *Aquaspirillum* and *Arthrobacter,* with the objectives of developing an adequate model to simulate bacterial transport and to improve our understanding of the mechanisms controlling bacteria transport through soils. Disturbed samples from an Alfisol topsoil and subsoil were used to fill 15 cm long soil columns. A pulse of bacterial suspension (initial concentration of 10^{11} cells ml^{-1}) was applied to the top of each soil column followed by the application of sterile water. Bacteria were counted in effluent portions and in soil using microscopy. Large variations were observed in the shape of breakthrough curves; effluent bacterial concentrations were occasionally larger than influent concentrations. We developed the 'limited entrapment model' to simulate the observed bacterial transport. The model assumes that (a) the capacity of soil pore space to trap bacteria is limited, (b) the bacteria entrapment rate depends on the amount of trapped bacteria and that the entrapment accelerates as the amount of trapped bacteria approaches the soil trapping capacity, and (c) the trapped bacteria form cell clusters that may be released back to the soil solution but travel slowly and may become re-trapped because of their size. The new model provided a satisfactory fit to data and underscored the importance of cell cluster formation for bacterial transport through soil.

K e y w o r d s:limited entrapment model, simulation, bacterial transport, soil columns

*Corresponding author's e-mail: ypachepsky@anri.barc.usda.gov
**The work was partially supported by NATO Collaborative Linkage Grant No. 979233 (NATO Science Programme, Cooperative Science & Technology Sub-Programme), Russian Foundation of Basic Research (RFBR) - Grants No. 01-04-48066, 04-04-49606, 03-04-48620, 03-04-48679 and 03-04-06703.

INTRODUCTION

Pathogenic bacteria, which may be released from land-applied manures or biosolids, are a critical issue for human health in some locations (Murphy and Ginn, 2000). Bacterial transport through soils is attracting a substantial attention because soil serves as an environmental bacterial filter. However, soils are not ideal filters. They are physically heterogeneous, and the presence of macropores and other preferential transport pathways may result in a rapid transport of bacteria directly to groundwater (Story *et al*., 1995; Natsch *et al*., 1996)

Bacteria are 'living colloids' (van Loosedrecht *et al*., 1989). Their comparatively large size limits their ability to be transported through the entire soil pore space. This is a part of the reason of bacterial entrapment or straining in rough soil pore spaces after bacteria have entered the soil with infiltrating water. Also, bacteria cell surfaces contain substances that work as glues providing means of attachment to soil particles (Quintero *et al*., 1998). Alternatively, bacteria can attach to surfaces via pili, flagella, *etc*. (Daniels, 1980; Newby *et al*., 1999). Bacteria also can form cell clusters that have much larger size and much lower mobility in soil compared with individual bacterial cells (Stoodley *et al*., 2000). The presence of water-air interfaces has been shown to affect bacterial transport in porous media (Powelson and Mills, 1996; 1998). Finally, soils have microbial ecosystems where bacteria may grow (depending on the presence of nutrients), dye-off (Corapcioglu and Haridas, 1984; 1985), or be subjected to predation. Consequently, bacterial transport through soils is a complex phenomenon affected by many variables.

Beginning from the seminal works of Nielsen and Biggar (1961, 1962), column experiments has become the established method to study the effect of soil physical and chemical heterogeneity on chemical and microbial transport in soils. Typically, the transported chemical/microbe is applied on the soil surface in the solution or suspension pulse that is preceded and followed with the contaminant-free solution. The influent concentration of the chemical or microbe sharply increases from zero to the level in the pulse when the pulse begins to enter soil column, and sharply decreases back to zero when the whole pulse enters the column. The effluent concentration demonstrates a graduate increase followed by a gradual decrease. The shape of the breakthrough curve *ie* the dependence of the effluent concentration on time or on cumulative effluent volume, is used to decide on the effect of soil heterogeneity on the chemical/microbial transport. For example, the presence of macropores or preferential transport is suggested if the chemical/microbe appears in the effluent much earlier than the average water infiltration rate suggests. A long tail of the breakthrough curve is usually associated with slow desorption kinetics or the presence of stagnant zones in pore space (Seuntients *et al*., 2001).

Breakthrough curves (BTC) of chemical tracers from the pulse experiments usually are unimodal, *ie* have a single maximum or a single 'flat top' range. Bacterial BTC are more complex and may have one more maximum (Ginn *et al*., 2002). A possible explanation of this is that bacteria may form cell clusters that are transported sporadically as opposed to the continuous transport observed with chemical compounds.

We conducted a series of *Aquaspirillum* and *Arthrobacter* transport experiments in soil columns and observed BTC having different shapes. The objective of this work was to develop an adequate model to simulate the observed BTC and to infer information about the mechanisms of the bacteria transport in soils from the modeling results.

MATERIALS AND METHODS

Arthrobacter sp. and *Aquaspirillum sp.* bacterial cultures were grown on agar medium containing 2 mg of peptone, 1 mg of glucose, 1 mg of yeast extract, and 1 mg of casein hydrolyzate per ml. *Arthrobacter* cells were coccal, 0.6-1.0 μm in diameter, without flagella. *Aquaspirillum* cells were spiral-shaped, were 1.4 μm long, with flagella. Cells were harvested from agar plates giving suspensions with concentrations of ca. 10^{12} cells ml^{-1}.

PVC columns, 5 cm in diameter and 15 cm long, were manually packed with disturbed, air-dried but not sieved samples of A (topsoil) and D (subsoil) horizons of the Alfisol soil from the Ivanovo region, Central Russia. Soil basic properties are given in Table 1. Soil samples were not sterilized prior to packing to prevent soil aggregate destruction.

T a b l e 1 . Selected soil properties

Soil horizon	Sand+silt (%)	Clay (%)	$C_{org.}$ (%)	Bulk density (g cm^{-3})	Water content (m^3m^{-3}) at different ψ*						
					0.48	0.70	1.00	1.30	1.70	4.51	5.16
A – Topsoil	72	28	0.86	1.36	0.482	0.454	0.413	0.389	0.362	0.025	0.011
D - Subsoil	94	6	nd	1.61	0.330	0.269	0.157	0.105	0.083	0.038	0.026

*ψ = soil matric potential, kPa; **nd - not determined.

Prior to transport experiments, soil columns were saturated with water from below for 1 day. First, 30 ml of sterile deionized water were applied to estimate infiltration rates (during 1 h for the topsoil samples and during 15 min for the subsoil samples) and the infiltration rate (Table 2). Then 200 ml of bacterial suspension was applied to the top of each column, and steady infiltration continued (the first phase of the experiment). As the bacterial suspension percolated through soil columns, sterile deionized water was applied (the second phase of the experiment). The experiment took 8 h for topsoil and 30 min for subsoil samples, respectively. All experiments were conducted at 15°C. Effluent samples were stored at 4°C to prevent bacterial growth. The initial infiltration rate (cm d^{-1}) data for each soil column are listed in the Table 2. There was an approximate 50% decrease in the infiltration rate, from 57.8 – 61.9 cm d^{-1} at the beginning of the experiment to 39.4 – 41.3 cm d^{-1} at the end, in topsoil columns. No reduction of infiltration rate was registered in subsoil columns. Columns were weighed after the experiment to estimate pore volume filled with water.

T a b l e 2. Soil column properties

Soil horizon	Column No.	Bulk density (g cm^{-3})	Infiltration rate (cm day^{-1})	Suspension pulse volume relative to pore volume
		Aquaspirillum sp.		
Topsoil	1	0.96	57.8	1.10
Topsoil	2	0.99	61.9	1.06
Subsoil	3	1.21	687.6	1.20
Subsoil	4	1.19	685.4	1.15
		Arthrobacter sp.		
Topsoil	5	0.97	57.8	1.07
Topsoil	6	0.98	46.8	1.09
Subsoil	7	1.20	670.8	1.19
Subsoil	8	1.19	599.6	1.17

Bacterial-soil specimens on slides were made from each 10 ml samples of effluent. Immediately after the experiment was completed, PVC columns were carefully separated from soil, and 2 mm thick slices of topsoil were cut from 0, 7.5, and 15 cm depths using a scalpel. Thin sections were observed directly under a microscope and photographed with a 'Zenith' camera with 480x magnification. One-g soil subsamples were examined from every 3 cm of columns. Each subsample was diluted with 100 ml of sterile deionized water, and the resulting soil suspensions treated with ultrasound for 1 min at 22 kHz. Slides were made from suspension probes after ultrasonic treatment, and bacterial concentrations counted as above. The background concentrations of native soil bacteria were obtained from experiments on leaching soil columns with sterile deionized water.

Enumerating microorganisms

Bacteria were counted under LUMAM-IZ fluorescent microscope with 480x magnification. The 0.1 mg l^{-1} solution of acrydine orange was used as a marker. Bacterial counts were converted to concentrations using the equation (Zvyagintsev, 1991):

$$M = \frac{4an}{p} 10^{10},$$

where: M is the concentration of bacteria (cells ml^{-1}), a is the average count of bacteria in the field of vision, p is the area of the field of vision (μm^2), and n is the dilution.

Each effluent specimen was characterized with 60 replications of bacterial counts. A total of 384 effluent specimens were counted.

RESULTS

Experimental data on bacterial transport

The statistical distributions for *Aquaspirillum* and *Arthrobacter* cell counts were mostly symmetrical; the median count value was within ±4% of the mean count value. The coefficients of variation of the counts were between 5 and 15 in 95% of all specimens. Mean counts are presented below.

Bacteria breakthrough data are shown in Fig. 1. In topsoil, the maximum *Aquaspirillum* concentration observed in breakthrough curves (BTC) occurred earlier than for *Arthrobacter;* both *Aquaspirillum* and *Arthrobacter* BTCs had one maximum. In subsoil, the breakthrough curves were bimodal; both first and second maxima for *Aquaspirillum* occurred earlier than for *Arthrobacter*. Maximum effluent concentrations of *Aquaspirillum* exceeded influent concentrations in both topsoil and subsoil columns.

Distributions of bacteria in soil are shown in Fig. 2. Bacteria contents increased with depth, and were one to two orders of magnitude larger at the 13.5 cm depth than at the 1.5 cm depth. No bacteria were detected at the depth of 1.5 cm in subsoil, whereas there were appreciable bacteria contents at this depth in topsoil.

The mass balance computations show that approximately 32% of the applied *Arthrobacter* cells and 28 to 38% of the *Aquaspirillum* cells were eluted from topsoil columns (Table 3). In subsoil columns approximately 44 to 68% for of applied *Arthrobacter* cells and 98 to 99% of *Aquaspirillum* cells were eluted.

Soil thin section photographs (Fig. 3) show that bacteria accumulated on the walls of large voids. The images from top thin sections (example in Fig. 3a) show a few single cells of bacteria (marked bright green) attached irregularly to soil particles. On the contrary, the imagery from thin sections from middle and, especially, the bottom of soil columns contained bright green spots much larger in size than in Fig. 3a. These spots were interpreted as bacterial cell clusters. As the fluorescence was very intensive on the thin sections from the bottom of columns, we assumed that this was due to bacterial colony formation or biofilms.

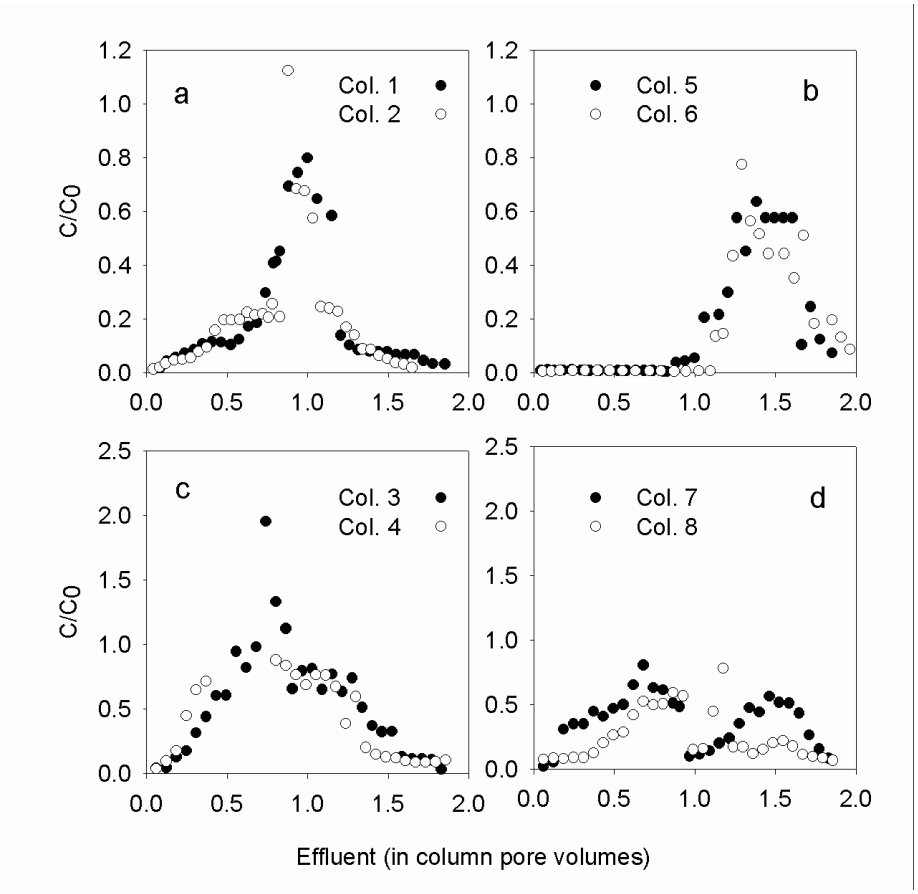

Fig. 1. Experimental bacterial breakthrough curves: a – *Aquaspirillum*, topsoil; b – *Aquaspirillum*, subsoil; c – *Arthrobacter*, topsoil; d – *Arthrobacter*, subsoil.

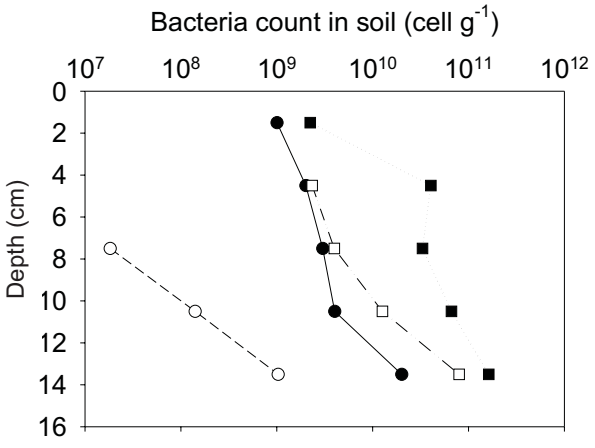

Fig. 2. Bacteria count in soil after experiment; ○ - *Aquaspirillum*, topsoil, □ - *Arthrobacter*, topsoil, ● - *Aquaspirillum*, subsoil, ■ - *Arthrobacter*, subsoil.

Modeling bacteria transport

The following assumptions were made to develop the bacteria transport model.

1. Soil has a limited trapping capacity such that no bacterial entrapment occurs after the capacity is reached. This assumption is made to explain the low cell concentrations in effluent at the earlier stages of the breakthrough curve when cells are entrapped vs. the increased cell concentrations in effluent at the later stages of the breakthrough curve when the trapping capacity has been exceeded.

2. The entrapment rate is a function of the number of entrapped bacteria. This assumption is made to explain the bimodality of the breakthrough curve. The entrapment rate is relatively slow when the number of entrapped bacteria are low, but increases as the number of entrapped bacteria approaches capacity due to a tendency of cells to adhere to colonies or biofilms. However, entrapment rate decreases again as capacity is exceeded. Consequently, the first maximum observed in break through curves is consistent with the initial slow entrapment rate, while the second maximum is consistent with achieving entrapment capacity.

T a b l e 3. Mass balance of bacteria in columns

Soil horizon	Column No.	Total number of applied bacteria, cells	S_1	S_{final}	S_{res}
			(%)		
		Aquaspirillum sp.			
Topsoil	1	$1.7\ 10^{13}$	11.9	38.9	35.4
Topsoil	2	$1.7\ 10^{13}$	0.7	27.9	ND
Subsoil	3	$1.7\ 10^{13}$	59.9	99.5	ND
Subsoil	4	$1.7\ 10^{13}$	72.9	98.0	1.5
		Arthrobacter sp.			
Topsoil	5	$9.2\ 10^{13}$	1.4	32.0	48.3
Topsoil	6	$9.2\ 10^{13}$	0.7	32.0	ND
Subsoil	7	$3.5\ 10^{13}$	37.8	68.0	ND
Subsoil	8	$3.5\ 10^{13}$	27.2	44.4	51.1

S_1 – bacteria that passed soil after one pore volume has been displaced; S_{final} – bacteria that passed soil by the end of the experiment; S_{res} – residual amount of bacteria in soil (column samples data).

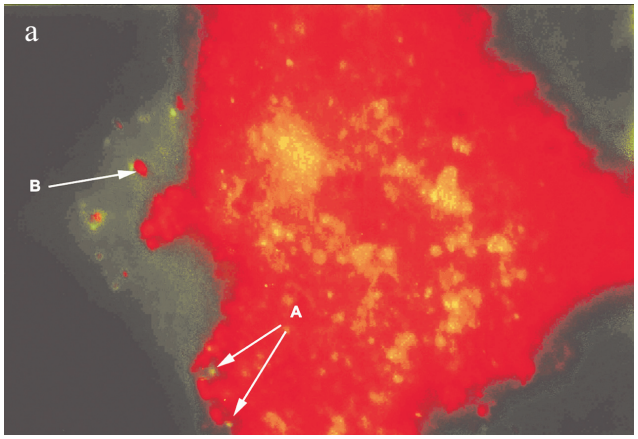

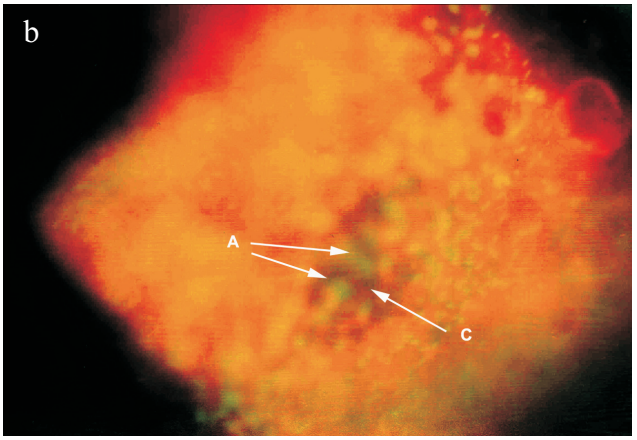

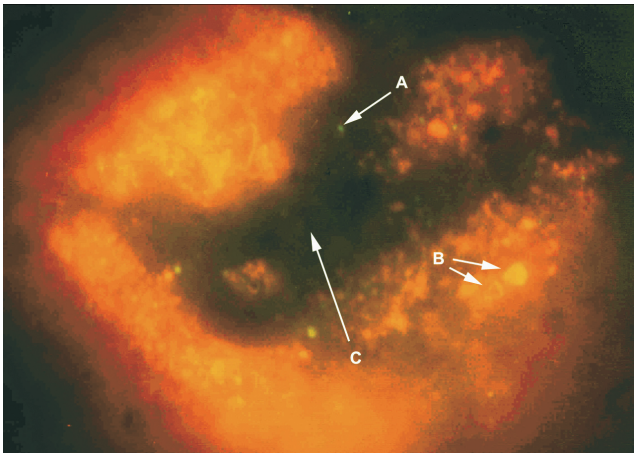

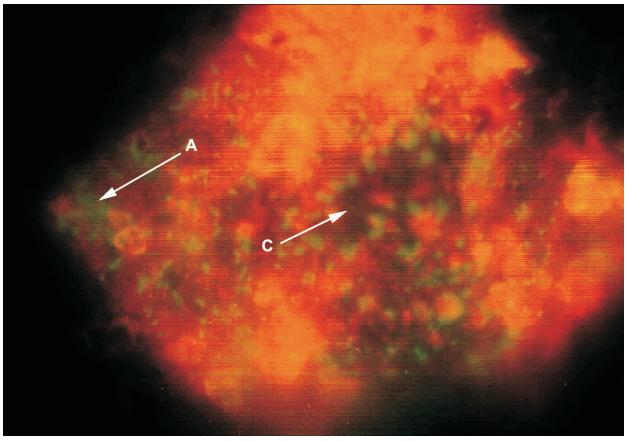

Fig. 3a. Thin-section images of bacteria in soil after the experiment – top of soil columns. A – bacteria; B – soil particles/microaggregates; C – pores; the images were obtained with the x480 magnification.

Fig. 3b. Thin-section images of bacteria in soil after the experiment – middle of soil columns. A – bacteria; B – soil particles/microaggregates; C – pores; the images were obtained with the x480 magnification.

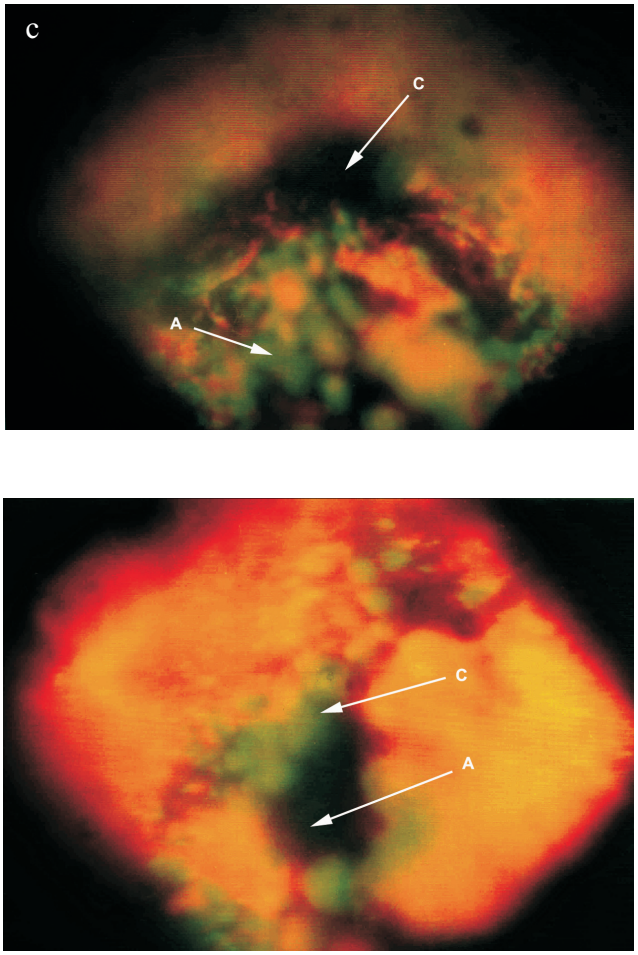

Fig. 3c. Thin-section images of bacteria in soil after the experiment – bottom of soil columns. A – bacteria; B – soil particles/microaggregates; C – pores; the images were obtained with the x480 magnification.

3. The entrapped bacteria can be released but they are released in cell clusters, as opposed to individual cells, that do not readily disintegrate. Furthermore, the transport of these cell clusters through the soil profile occurs separately from that of individual cells. Specifically, cell clusters tend to travel shorter distances through soil before being intercepted due to their larger size. The ramifications of this are two-fold: i) the distribution of bacteria in the soil profile are skewed with relatively fewer numbers in the top and greater numbers at the bottom, and ii) effluent bacterial concentrations occasionally exceed influent concentrations due to the periodic elution of cell clusters (large cell numbers in a relatively small volume).

The three assumptions are included in the following equations of the model. The convective-dispersive model with entrapment term is used to simulate the bacteria transport in saturated soil column:

$$\theta_1 \frac{\partial C}{\partial t} = D^* \frac{\partial^2 C}{\partial x^2} - q_1 \frac{\partial C}{\partial x} - \mu C; \; \rho \frac{\partial S}{\partial t} = \mu C, \qquad (1)$$

where: θ_1 is the soil water content in pore space available for bacteria, $cm^3 cm^{-3}$, C is the concentration of individual bacterial cells in soil solution, count cm^{-3}, t is time, D^*, is the dispersion coefficient , $cm^2\ h^{-1}$, x is the distance from top of the column, cm, q_1 is the water flux in the zone available for bacteria, cm h^{-1}, μ is the bacteria entrapment rate, h^{-1}, ρ is the soil bulk density, g cm^{-3}, S is the trapped bacteria content, count (g of soil)$^{-1}$.

It is convenient to use dimensionless variables:

$$c = \frac{C}{C_o}; \tau = \frac{qt}{\theta L}; D = \frac{\theta}{\theta_1}\frac{D^*}{qL}; z = \frac{x}{L}; v = \frac{\theta}{\theta_1}\frac{q_1}{q};$$
$$b = \frac{\theta}{\theta_1}\frac{\mu L}{q}; s = \frac{\rho S}{\theta_1 C_o}, \qquad (2)$$

where: C_O is the bacteria concentration in the influent, c is the relative bacteria concentration, θ is the soil water content, q is the soil water flux, τ is the cumulative water flux divided by the total pore volume of the column; when applied to breakthrough curves of a column, value of τ is the effluent volume measured in numbers of column pore volumes; this value shows how many times the pore water was displaced by the influent solution, D is the dimensionless dispersion coefficient, z is the dimensionless distance measured with relation to the column length, z=1 at the bottom of the column, í is the dimensionless pore water velocity; it is the ratio of the pore water velocity in pores available for bacteria (q_1/θ_1) to the average pore water velocity (q/θ); b is the dimensionless bacteria entrapment rate, s is the dimensionless bacteria content in soil; this is the ratio of the bacteria content per gram of soil to bacteria content in the bacteria-available pore volume corresponding to 1 g of soil and filled with the influent.

Using the dimensionless variables (2), one transforms Eq. (1) to:

$$\frac{\partial c}{\partial \tau} = D\frac{\partial^2 c}{\partial z^2} - v\frac{\partial c}{\partial z} - bc; \qquad \frac{\partial s}{\partial t} = bc. \qquad (3)$$

The entrapment rate is made dependent on the content of trapped bacteria in this work. The dependence is:

$$b = \begin{cases} b_{\min} + b_c s^n, & s < s_{\max} \\ 0, \text{ if } s \text{ has reached } s_{\max} \end{cases}. \qquad (4)$$

Here the parameter s_{max} is the soil trapping capacity with respect to the bacteria in question. This is the maximum content of entrapped bacteria that can be reached. The parameter b_{min} is the initial entrapment rate that is applicable at early stages of transport when only background

bacteria were present and transport-related entrapment has occurred. The parameter b_c is responsible for increase of the entrapment rate with the increase in trapped bacteria amount; for the same trapped amount s and bacteria concentration in solution, the larger b_c is, the faster bacteria will be trapped. The parameter n is responsible for the acceleration of the entrapment with the increase of the trapped amounts. The trapping rate growth linearly with the trapped amount when n=1. The trapping rate accelerates with growth of s when n>1. The trapping rate shows some retardation when n<1.

The system of Eqs (3) and (4) was solved with the initial conditions $c(z,0)=c_i$, $s(z,0)=0$ and boundary condition $c(0,\tau)=1$ and $c(0,\tau)=1$ for $\tau > \tau_p$ and $\tau < \tau_p$, respectively, τ_p is the volume of the bacteria influent pulse divided by the column pore volume, c_i is the background concentration. The lower boundary was set at z=5, and the boundary condition $c(5,\tau)=0$ was maintained. The explicit finite difference scheme was used in the numerical solution. The accuracy of the numerical solution was tested using the analytical solution of the Eq. (3) with constant value of b as described by van Genuchten (1985). Maximum 0.5% difference between numerical and analytical solution was observed (data not shown). The Marquardt algorithm as described by van Genuchten (1981) was applied to fit the numerical solution of (3) and (4) to the experimental data.

We varied parameters of the model (3) and (4) and simulated the bacteria breakthrough to illustrate the effect of the entrapment model parameters s_{max}, b_{min}, b_c, and n of the on the shape of the BTC. Values of ν=2.5, D=0.5, and τ_p = 1.2 were used in all these simulations. The simulated breakthrough curves are shown in Fig. 4. The companion Table 4 contains the parameter sets of each of curves.

The effect of the trapping capacity on the simulated BTC is shown in Fig. 4a. All simulated BTC are bimodal. The trapping rate accelerates as the trapped amount approaches s_{max}, and that causes the first maximum to occur. The second BTC maximum decreases as the value of s_{max} increases. More bacteria appear to be trapped in the column and less bacteria appear to be available to form second BTC maximum as the value of s_{max} increases.

The effect of the initial entrapment rate rate b_{min} on the simulated BTC is shown in Fig. 4b. The trapping capacity is not reached with the small initial entrapment rate b_{min}=0.2, and bacteria are transported mostly in the solution. The breakthrough is unimodal, and the BTC almost repeats the input concentration pulse, with slight modifications caused by dispersion and trapping. The trapping capacity is reached with intermediate and high initial entrapment rates. The bimodal breakthrough with two comparable peaks is simulated with the intermediate initial entrapment rate b_{min}=2. The high initial entrapment rate b_{min}=20 generates the bimodal breakthrough with the first peak substantially lower than second. The first peak reflects the fast trapping of the first portions of bacteria entering the column. The second peak reflects the passage of the later portions of bacteria that are not affected by trapping anymore because the trapping capacity is reached.

The effect of the parameter b_c on the BTC is shown in Fig. 4c. The low value b_c=10 causes the filling of the trapping capacity at late stages of the breakthrough. The BTC is unimodal and is narrower than the influent pulse; its tail is 'eaten' by the trapping. The high value of b_c=250 causes most of trapping to occur at early stages of breakthrough. The second peak is completely unaffected by the trapping and the maximum effluent concentrations are close to the concentrations in the influent.

The effect of the acceleration parameter n on BTCs is shown in Fig. 4d. As the value of n decreases, less acceleration in trapping occurs when the trapped amounts increase. The first peak becomes smaller as the value of n grows lower than n, and an almost unimodal BTC is seen with n=0.5. Its rising limb appears when τ is close to 1, and, using the usual reasoning about breakthrough of chemicals in soils, one could assume that either the whole pore space is available for bacteria or adsorption occurs simultaneously with bacteria exclusion. However, one would be then lost to wonder why the pulse width is substantially less than the width of the influent pulse.

One substantial simplification of the limited entrapment models occurs when the value of b_c is set to zero. Then the model (4) contains only two parameters – s_{max} and b_{min}, because the value of n does not matter anymore. Simulated BTC are shown in Fig. 4d. They are all unimodal. Small values of b_{min} do not allow trapped bacteria amounts to reach the trapping capacity. When the b_{min} becomes large enough, the BTC front is 'eaten away' by trapping.

Data in Fig. 4 show that BTC shapes similar to the experimental BTC in Fig. 1 can be simulated with the proposed models. Graphs in Fig. 4 were used to select initial estimates for the parameters in fitting the model to the measured BTC. Results of fitting are shown in Fig. 5. Fitting the model to datasets for *Aquaspirillum* in the column 2 and *Arthrobacter* in the column 6 in topsoil were not successful, because the fitting algorithm tended to get stuck in a local minimum. Therefore, parameters for the second replication (*Aquaspirillum* column 1 and *Arthrobacter* column 5) were used to plot the simulated BTC for *Aquaspirillum* column 2 and *Arthrobacter* column 6 experiments. A generally good fit was observed, although the occasional values of relative effluent concentrations larger than one could not be simulated.

The parameter values are shown in Table 5. The trapping capacity of the topsoil is larger than that of the subsoil; the trapping capacity is higher for the *Arthrobacter* as compared with *Aquaspirillum* in both soil horizons. The initial trapping rate is higher in topsoil as compared with subsoil for each of bacteria. Values of parameter n are unity or larger and provide the acceleration of trapping rate as the trapped numbers increase.

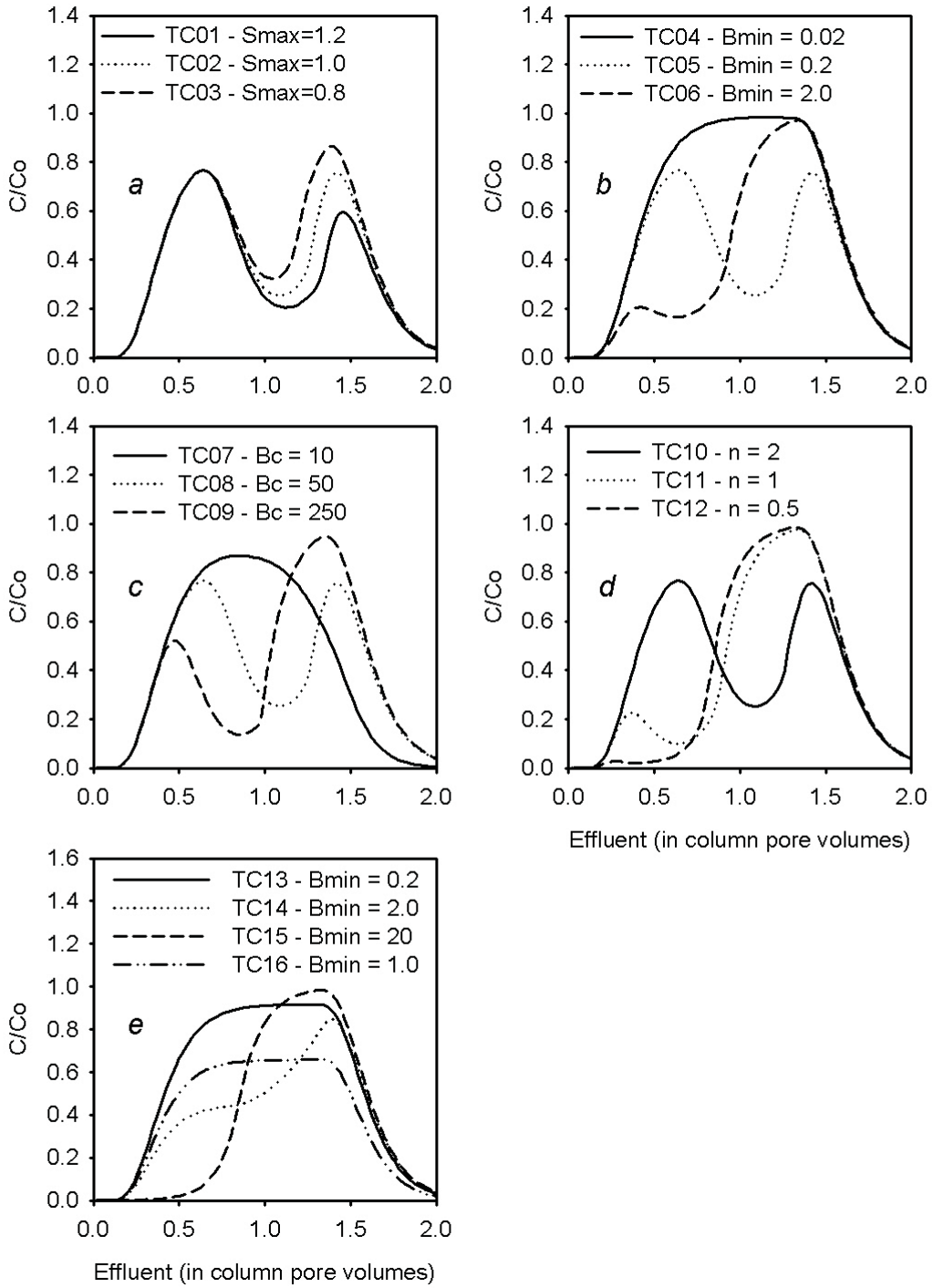

Fig. 4. Breakthrough curves simulated with the limited entrapment model. TC – test case. Parameter sets of each of the test cases are in the companion Table 4. Explanations to a–e see the text.

T a b l e 4. Parameters of the limited entrapment model for the test cases in Fig. 3

Test case (TC)	b_{min}	b_c	n	s_{max}
01	0.2	50	2.0	1.2
02	0.2	50	2.0	1.0
03	0.2	50	2.0	0.8
04	0.02	50	2.0	1.0
05	0.2	50	2.0	1.0
06	2.0	50	2.0	1.0
07	0.2	10	2.0	1.0
08	0.2	50	2.0	1.0
09	0.2	250	2.0	1.0
10	0.2	50	2.0	1.0
11	0.2	50	1.0	1.0
12	0.2	50	0.5	1.0
13	0.2	0	2.0	1.0
14	2.0	0	2.0	1.0
15	20.0	0	2.0	1.0
16	1.0	0	2.0	1.0

T a b l e 5. Parameters of the limited entrapment model for experimental breakthrough curves

Bacteria	Horizon*, column	v	D	b_{min}	b_c	n	s_{max}
Aquaspirillum	T1, T2	1.7	0.4	20	50	1.0	1.07
Arthrobacter	T5, T6	4.7	12	22	1300	13.0	1.47
Aquaspirillum	S3	2.4	1.2	0.14	20	3.8	0.17
Arthrobacter	S4	2.0	1.2	0.3	120	21.0	0.42
Aquaspirillum	S7	2.1	0.4	5.1	365	2.0	0.82
Arthrobacter	S8	1.5	0.8	0.1	43	1.5	0.73

*T – topsoil, S - subsoil.

DISCUSSION

There was a substantial difference in the transport of *Aquaspirillum* and *Arthrobacter* through soil columns (Fig. 1). Specifically, the maximum cell concentrations observed in break through curves occurred earlier with *Aquaspirillum* than with *Arthrobacter*. The fact that *Aquaspirillum* are motile while *Arthrobacter* are non-motile suggests that motility is an important variable affecting bacterial transport. In addition to motility, cell shape, hydrophobicity and surface charge, and/or cell surface chemistry have been proposed to affect bacterial transport (Fletcher, 1996), although the data are inconclusive. For example, Camper *et al*., (1993) did not observe any effect of *Pseudomonas fluorescens* motility on their breakthrough in glass-bead columns. On the contrary, Camesano and Logan (1998) reported an effect of bacteria motility on transport in saturated soil columns, and suggested that swimming cells were presumably able to avoid sticking to soil grains at low fluid velocities, but at higher fluid velocities cell motility did not reduce attachment. Gannon *et al*., (1991) did not find any correlations between transport rates for 19 bacterial strains through soil or their retention by this soil and cell hydrophobicities or net surface charges. On the other hand, Gross and Logam (1995) observed that the number of *A. paradoxus* retained by the porous media was decreased by treatments that made bacteria more hydrophobic and less electrostatically charged. Consequently, the effect of different cell properties on transport rates remains elusive.

In this study, bacterial breakthrough in sandy subsoil was more pronounced as compared to in silt loam topsoil (cf. Figs 1a and c, 1b and d). Both soil surface charge and structure of soil pore space *ie* arrangement of particles, could cause this difference (Dong *et al*., 2002; Jamieson, 2002). Larger differences in bacteria breakthrough were caused by the soil than by the bacteria genus. The differences in soil structure probably created different opportunities for bacteria entrapment. The topsoil should have more complex structure resulting in larger values for soil trapping capacity s_{max} and initial trapping rate b_{min} (Table 5).

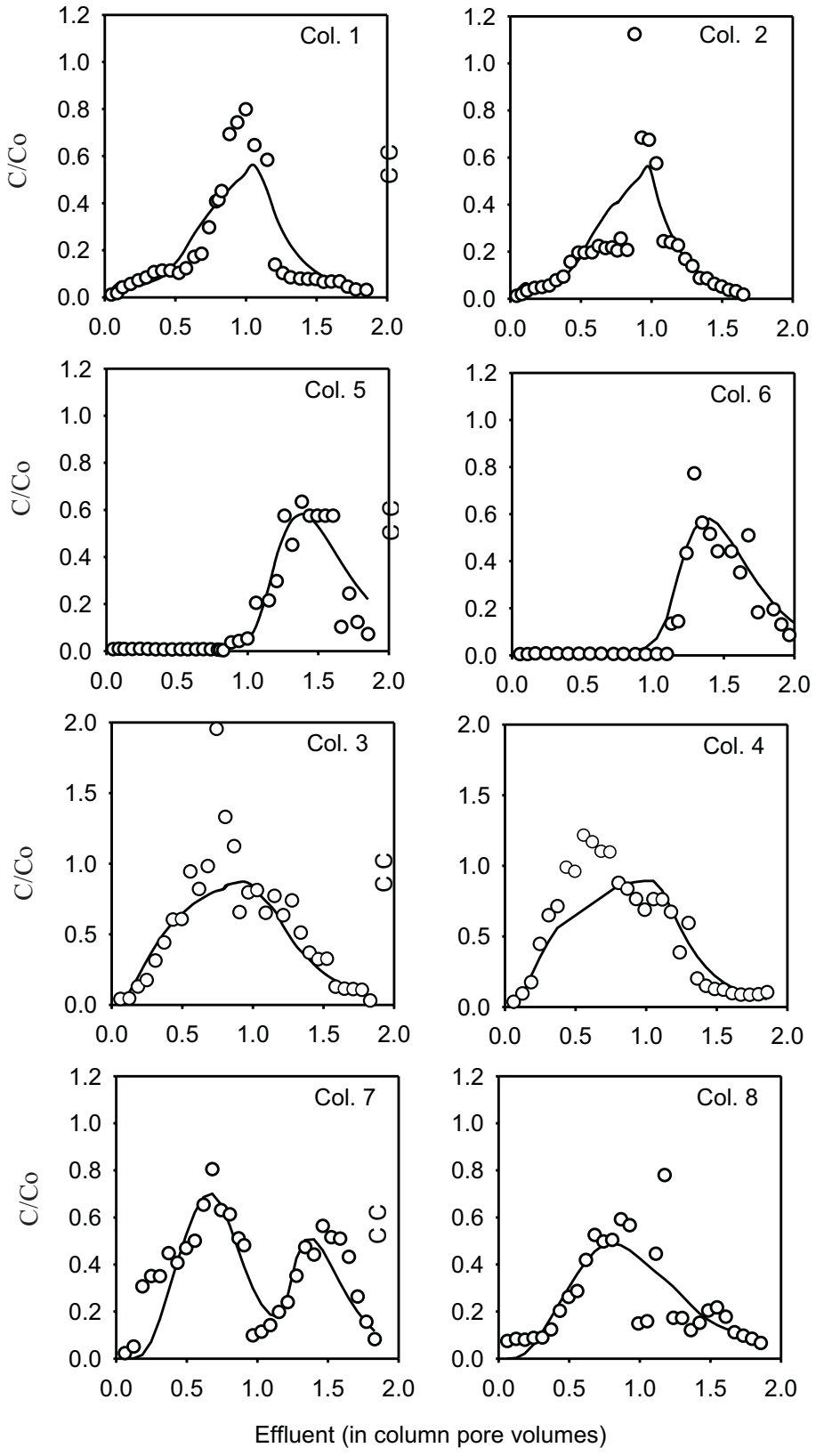

Fig. 5. Best fits of the limited entrapment model to the experimental breakthrough.

Some effluent concentrations were higher than in the influent. This was more common in the sandy subsoil. The flow in subsoil columns was much more rapid where soil structure was relatively simple. That created more opportunities for cell clusters to reach the column outlet, as compared with topsoil columns with more complex structure and unstable (slacking) soil aggregates. Cell clusters and their concentrations increased with depth (Fig. 3) such that only relatively small clusters passed through the entire column. Transport of single bacteria cells is restricted by the available pore space. Bacterial cells are physically excluded from the micropores (Newby *et al*., 1999). In terms of matric potential, bacteria cannot pass the pore necks if the neck diameter corresponds to a soil matric potential of -147 kPa (Griffin and Luard, 1979). This value corresponds to an average diameter of 1 μm or less. The observed clusters were mostly larger than that (Fig. 3) and therefore would have much less pore space to move through. That may explain the fact that concentrations in the effluent, albeit larger than in influent, did not exceed the concentrations in influent significantly.

Bacterial cell cluster formation is known to be affected by various environmental factors (Hall-Stoodley and Stoodley, 2002). Therefore, the actual importance of cell cluster formation for transport may be affected by specific soil conditions. Cell cluster formation may appear to be beneficial or harmful if bacterial transport is used in technological purposes, *eg* for bioremediation. There may be a potential of the additional control of the transport by enhancing or eliminating cell cluster formation.

Bimodal breakthrough of chemicals in soils is often interpreted using models which assume two independent pore spaces (Lennartz *et al*., 1997; Garrido *et al*., 2001). This model represents BTC by averaging two BTCs resulting from the transport in two pore subspaces conducting water and solutes with two different velocities. This model appeared to be inapplicable to our dataset (data not shown), because the simulated BTC in each of the subspaces had widths approximately the same as the width of the influent pulse. Therefore, the average BTC had a total width larger than the input pulse. The bimodal BTCs for *Arthrobacter* in subsoil had an average width approximately equal to the width of the influent pulse.

The bacteria transport in solution model developed in this work should be complemented with the transport model for trapped cell clusters to simulate data in Fig. 2. However, additional experiments with different transport times and/or pulse durations are needed. Such experiments present an interesting avenue for developing a better understanding of the role of cell cluster formation on bacteria transport in soils.

We realize that these modeling results do not present a proof that the mechanisms of bacterial transport in the experiments were the same as suggested in this work. There may be other plausible set(s) of hypotheses to explain the bimodal bacteria breakthrough. Nevertheless, results of this work seem to underscore the need for considering bacteria cell cluster formation as one of the potentially important mechanisms of bacteria transport in soil.

CONCLUSIONS

1. Large variations were observed in the shape of breakthrough curves *Aquaspirillum* and *Arthrobacter* obtained from column experiments with an Alfisol topsoil and subsoil. Effluent bacterial concentrations were occasionally larger than influent concentrations.

2. The 'limited entrapment' model was developed to simulate the observed bacterial transport. The critical assumptions of the model were that (a) the capacity of soil pore space to trap bacteria is limited, (b) the bacteria entrapment accelerates as the amount of trapped bacteria approaches the soil trapping capacity, and (c) the trapped bacteria form cell clusters that may be released back to the soil solution but travel slowly and may become re-trapped. The model provided a satisfactory fit to the data.

3. The trapping capacity of the topsoil was larger than that of the subsoil. The trapping capacity was higher for the *Arthrobacter* as compared with *Aquaspirillum* in both soil horizons. The initial trapping rate was higher in topsoil as compared with subsoil for both bacteria.

4. Bacteria cell cluster formation is one of the potentially important mechanisms of bacteria transport in soil.

REFERENCES

Camesano T. and Logan B.E., 1998. Influence of fluid velocity and cell concentration on the transport of motile and nonmotile bacteria in porous media. Environ. Sci. Technol., 32, 1699-1708.

Camper A.K., Hayes J.T., Sturman P.J., Jones W.L., and Cunningham A.B., 1993. Effects of motility and adsorption rate coefficient on transport of bacteria through saturated porous media. Appl. Environ. Microbiol., 59, 3455-3462.

Corapcioglu M.Y. and Haridas A., 1984. Transport and fate of microorganisms in porous media: A theoretical investigation. J. Hydrol., 72, 149-169.

Corapcioglu M.Y., and Haridas A., 1985. Microbial transport in soils and groundwater: A numerical model. Adv. Water Resour., 8, 188-200.

Daniels S.L., 1980. Mechanisms involved in sorption of microorganisms to solid surfaces. In: Sorption of Microorganisms to Surfaces (Ed. G. Bitton and K.C. Marshall). John Wiley & Sons, Inc., New York, NY.

Dong H., Onstott T.C., DeFlaun M.F., Fuller M.E., Streger S.H., Rothmel R.K., and Mailloux B.J., 2002. Relative dominance of physical vs. chemical effects on the transport of adhesion deficient bacteria in intact cores South Oyster, VA. Environ. Sci. Technol., 36, 891-900.

Fletcher M., (Ed.), 1996. Bacterial Adhesion: Molecular and Ecological Diversity. Wiley-Liss, New York, N.Y.

Gannon J.T., Manilal V.B., and Alexander M., 1991. Relationship between cell surface properties and transport of bacteria through soil. Appl. Environ. Microbiol., 57, 190-193.

Garrido F., Ghodrati M., Campbell C.G., and Chendorain M., 2001. Detailed characterization of solute transport in a heterogeneous field soil. J. Environ. Qual., 30, 573-583.

Ginn T.R., Wood B.D., Nelson K.E., Scheibe T.D., Murphy E.M., and Clement T.P., 2002. Processes in microbial transport in the natural subsurface. Adv. Water Resour., 25, 1017-1042.

Griffin D.M. and Luard E.J., 1979. Water stress and microbial ecology. In: Strategies of Microbial Life in Extreme Environments (Ed. M. Shilo). Berlin, Dahlem Konferenzen, 49-63.

Gross M.J. and Logan B.E., 1995. Influence of different chemical treatments on transport of *Alcaligenes paradoxus* in porous media. Appl. Environ Microbiol., 61, 1750-1756.

Hall-Stoodley L. and Stoodley P., 2002. Developmental regulation of microbial biofilms. Curr. Opin. Biotechnol., 13, 228-233.

Jamieson R.C., Gordon R.J., Sharples K.E., Stratton G.W., and Madani A., 2002. Movement and persistence of fecal bacteria in agricultural soils and subsurface drainage water: A review. Canadian Biosystems Eng., 44, 1.1-1.9.

Lennartz B., Kamra S.K., and Meyer-Windel S., 1997. Field scale variability of solute transport parameters and related soil properties. Hydrol. Earth Syst. Sci., 4, 801-811.

Murphy E.M. and Ginn T.R., 2000. Modeling microbial processes in porous media. Hydrogeol. J., 8, 142-158.

Natsch A., Keel C., Troxler J., Zala M., von Albertini N., and Defago G., 1996. Importance of preferential flow and soil management in vertical transport of a biocontrol strain of *Pseudomonas fluorescens* in structured field soil. Appl. Environ. Microbiol., 62, 33-40.

Newby D.T., Pepper, I.L., and Maier R.M., 1999. Microbial transport. In: Environmental Microbiology (Eds R.M. Maier, I.L. Pepper, and C.P. Gerba). Academic Press, San Diego, USA.

Nielsen D.R. and Biggar J.W., 1961. Miscible displacement in soils: I. Experimental information. Soil Sci. Soc. Am. Proc., 25, 1-5.

Nielsen D.R. and Biggar J.W., 1962. Miscible displacement in soils: III. Theoretical considerations. Soil Sci. Soc. Am. Proc., 26, 216-221.

Powelson D.K. and Mills A.L., 1996. Bacterial enrichment at the gas-water interface of a laboratory apparatus. Appl. Environ. Microbiol., 62, 2593-2597.

Powelson D.K. and Mills A.L., 1998. Water saturation and surfactant effects on bacterial transport in sand columns. Soil Sci., 163, 694-704.

Quintero E.J., Busch K., and Weiner R.M., 1998. Spatial and temporal deposition of adhesive extracellular polysaccharide capsule and fimbriae by *Hypnomonas* strain MHS-3. Appl. Environ. Microbiol., 64, 1246-1255.

Seuntjens P., Mallants D., Cornelis C., and Geuzens P., 2001. Nonequilibrium cadmium leaching in layered sandy soils. Soil Sci., 166, 507-519.

Stoodley P., Hall-Stoodley L., and Lappin-Scott H.M., 2000. Detachment, surface migration and other dynamic behavior in bacterial biofilms revealed by digital time-lapse imaging. Methods Enzymol., 337, 306-319.

Story S.P., Amy P.S., Bishop C.W., and Colwell F.S., 1995. Bacterial transport in volcanic tuff cores under saturated flow conditions. Geomicrobiol. J., 13, 249-264.

Updegraff D.M. and Wren G.B., 1954. The release of oil from petroleum-bearing materials by sulfate-reducing bacteria. Appl. Microbiol., 2, 309-322.

Van Genuchten M.Th., 1981. Non-equilibrium transport parameters from miscible displacement experiments. Research Rep. No. 119. U.S. Salinity Laboratory, USDA-SEA-ARS, Riverside, CA.

Van Genuchten M.Th., 1985. Convective-dispersive transport of solutes involved in sequential first-order decay reactions. Computers & Geosciences, 11, 129-147.

van Loosdrecht M.C.M., Lyklema J., Norde W., and Zehnder A.J.B., 1989. Bacterial adhesion: A physicochemical approach. Microb. Ecol., 17, 1-15.

Zvyagintsev D.G. (Ed.), 1991. Methods of Soil Microbiology and Biochemistry. Moscow University Publishers, Moscow, Russia (in Russian).